Flow Visualisation of Three-Dimensional Effects in a Cavity Flow

K. Schumacher, R. Kelso and C. Doolan

School of Mechanical Engineering
University of Adelaide, Adelaide, South Australia 5005, Australia

Abstract

This paper discusses visualisation of three-dimensional flow about a cavity at low Reynolds number. The length-to-depth ratio was six while the length-to-span ratio was three, classifying it as an open, three-dimensional cavity flow, typical of an aircraft weapons bay. The paper discusses the interaction of the shear/mixing layer with the side wall of the cavity. At very low Reynolds number the thickness of the mixing layer over the cavity is significant compared with the span of the cavity. Therefore, a mixing region with a periodic structure forms at the sides of the cavity. The main original finding is that this structure is explained by the interaction of sequential shear layer vortices with each other, with the side wall of the cavity and with the flat plate adjacent to the side of the cavity.

Introduction

A cavity flow consists of a backward-facing-step flow followed by a forward-facing-step flow. Cavities which are narrow, or three-dimensional, are defined as having $L/W > 1$, where L is the cavity length and W is the cavity span [1, p. 42]. Narrow cavities are typical geometries for aircraft weapons bays and landing gear wells. They may also be required geometries on other land and air vehicles of various forms.
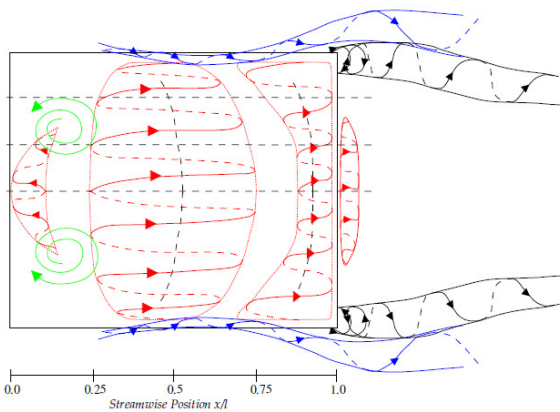

Figure 1: Sketch of flow structure around a three-dimensional cavity given by Knowles, Ritchie and Lawson, [6]. Plan view. Flow from left to right. Reproduced with permission.

When the cavity is narrow, three-dimensional effects may be significant. Mean in-flow and out-flow processes have been identified across the side boundaries of the cavity. In a study of a low Reynolds number flow, Crook, Kelso and Drobik [4] identified 'weak lateral flow' into the cavity in the upstream part and 'stronger lateral flow' out of the cavity in the downstream part. Crook et al. [4] also identified a possible vortex emanating from each rear corner of the cavity. Crook et al. [4] considered there to be a net in-flow from the shear layer impingement which is balanced by the out-flow of fluid along the downstream end boundaries.

Similar time-average flow patterns have been proposed for high Mach number, high Reynolds number flows relevant to practical applications [2,3,6] as for these low Reynolds number flows. Figure 1 shows a sketch of the flow structure around a three-dimensional cavity at Mach 0.85 as interpreted by Knowles, Ritchie and Lawson [6]. The identified features (such as upright vortices in the upstream part of the cavity, recirculation zones, separation downstream of the cavity trailing edge and features emerging from the corners and sides of the cavity) are typical of those found in even low Reynolds number flows.

In a recent study, Zhang and Naguib [9] identified that strong pressure oscillations near the cavity side walls were due to secondary flow patterns in the region. In most other studies the side walls and adjacent flat plate were not within the zone of measurement, or the cavity was flush with the walls of the wind or water tunnel. Therefore few other studies to date have focussed on the unsteady flow created by the presence of a side wall and adjacent flat plate, despite such three-dimensional effects being significant for narrow cavities. The present paper thus discusses some original experimental observations of the underlying flow structure about the flat plate adjacent to the sides of the cavity.

Experimental Method

This study is subsequent to earlier work conducted by Crook et al. [4] and Crook, Hassan & Kelso [3]. Using the experimental model built by Crook et al. [3], experiments were conducted in a water tunnel with cross-sectional dimensions of 0.5 m by 0.5 m. This experimental model is sketched in figure 2. A spanwise dye slot of 0.8mm width has been added, located 210mm upstream of the cavity. The cavity with geometry of L=450mm, D=75mm (where D is the cavity depth) and W=150mm was tested at a free-stream flow velocity of U=40mm/s. This gave a depth-based Reynolds number of 2700. At the cavity leading edge, there was a laminar boundary layer with estimated thickness δ_0=15mm and estimated momentum thickness θ_0=2.0mm (θ_0/D=2.7×10^{-2}).
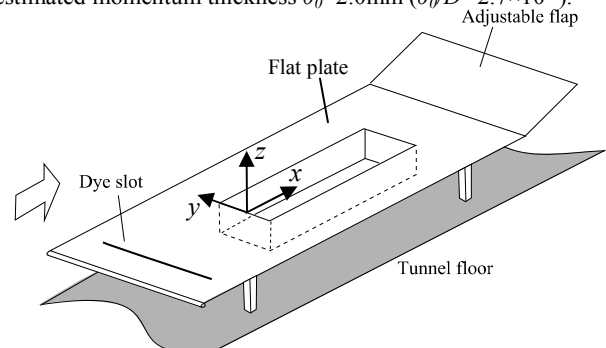

Figure 2: Sketch of experimental model, with location of dye slot indicated.

Additional measurements were taken in an open-jet wind tunnel using a 43% scale version of the water tunnel model. The free stream velocity was U=3m/s (turbulence intensity < 1%) with L=194mm, D=32mm and W=68mm, giving a depth-based Reynolds number of 6400. The accumulated contraction boundary layer was redirected under a circular nose profile.

There was no circulation control flap. The cavity leading edge boundary layer was measured to be approximately δ_0=8.0mm thick with a shape factor, approximately H=2.0. The momentum thickness was θ_0=1.0mm so that θ_0/D=3.1×10^{-2}.

Results and Discussion

Identification of dye pattern

Figure 3 shows the typical dye pattern formed as dye is released from the upstream slot. The structures in the shear layer are periodic and highly three-dimensional. Two shear layer vortices can be seen orientated across the span of the cavity. Although it will take a certain time for the streaklines to reveal the presence of a vortical feature [5], it appears that, at this Reynolds number, there is significant curvature to what is usually referred to as the 'spanwise roller' shear layer vortex. Indeed the vortex does not appear to attach to the side walls of the cavity until approximately one-half of the cavity length in this case.
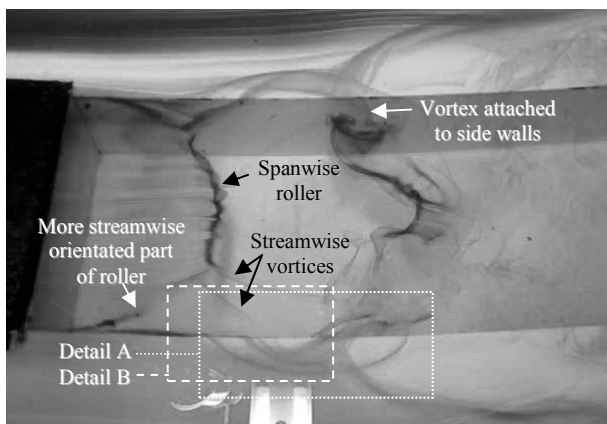

Figure 3: Typical dye pattern formed when dye is introduced from a slot upstream of the cavity. Flow from left to right. View: $0 \leq x/L \leq 0.8$.

Figure 3 also shows possible streamwise [8] (or 'strain-orientated' [7]) vortices near the upstream shear layer vortex. These form in-between the 'spanwise rollers' in the region of high strain [7].

The thickness of the shear layer is considerable compared to the width (and depth) of the cavity at this Reynolds number. Thus a three-dimensional shear region is formed as the growing mixing layer interacts with the flat plate adjacent to the cavity. In this region, the more streamwise-orientated part, or 'leg', of the shear layer 'spanwise roller' vortex (see figure 3) appears to exit the cavity over the sides (this is shown more clearly in figure 7).

A distinctive tornado-like vortex forms at regular intervals adjacent to each spanwise roller. This vortex is indicated by the arrow in figure 4 (in order to obtain a clearer photograph, the circulation control flap was adjusted so that the feature was stronger than usual). This vortex appears to carry fluid up from the flat plate surface. The vortex then turns towards the centreline and then down into the cavity.

Figure 5 shows the distinctive instantaneous dye pattern formed adjacent to the cavity. In the figure, lighter coloured regions on the flat plate would tend to suggest either more diffusion has occurred or fluid is transported laterally and replaced by undyed fluid. The tornado-like vortex can be seen and is marked by a curved arrow which indicates the direction of circulation of the vortex. Also there is an inner edge visible containing a lighter coloured region. There is additionally an outer edge containing darker fluid. Located downstream, the edge of the previous cycle of this pattern can be seen—this marked region of fluid has continued to grow outwards as it travels downstream.
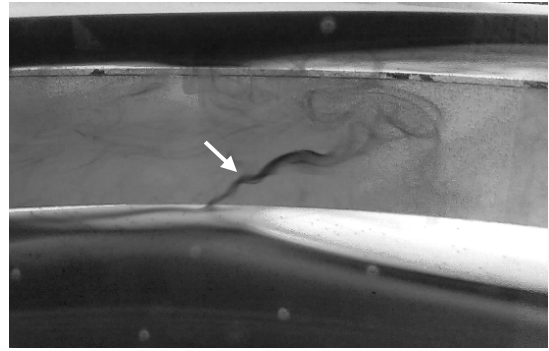

Figure 4: Arrow indicates tornado-like vortex formed at sides of cavity. Flow is from left to right. Vortex located on near side (to camera) of flat plate adjacent to cavity. Oblique view covering, approximately, $0.2 \leq x/L \leq 0.7$.
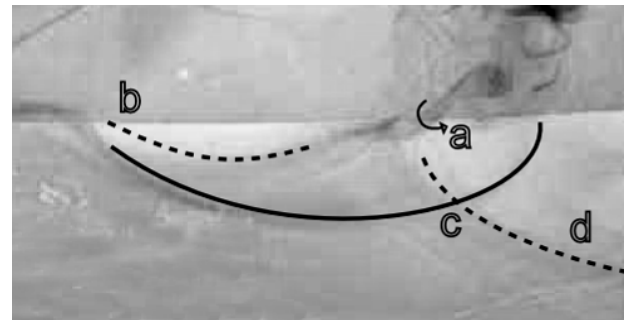

Figure 5: Dye pattern formed at side of cavity. Flow is from left to right. Field of view as per 'Detail A' on figure 3. (a) Tornado-like vortex. (b) Edge of inner, lighter region. (c) Edge of outer, darker region. (d) Previous cycle of this pattern, having convected downstream.
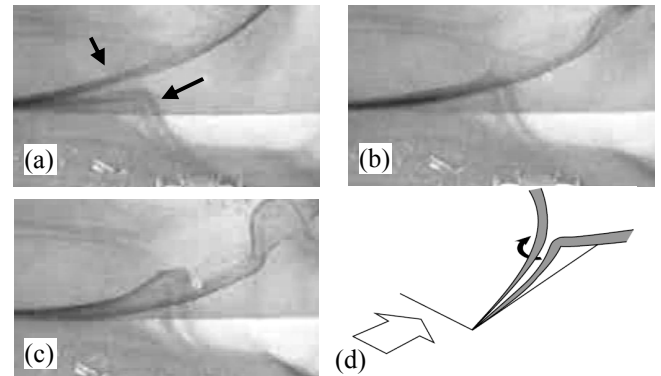

Figure 6: Interaction of sequential vortices. From from left to right. (a)-(c) Video frames, view as per 'Detail B' on figure 3. (d) Sketch.

Figure 11 shows a cut-away sketch of the instantaneous dye visualization pattern of figure 3. In the sketch, the main features that have been discussed are summarised.

Explanation for dye pattern

Figure 6(a)-(c) shows a series of video frames which illustrate the interaction of the stream-wise orientated portions, or 'legs', of the shear layer vortices. The earlier leg (believed to be the 'kinked' shaped region of dye) appears to be drawn under and around the leg of the later shear layer vortex as sketched in figure 6(d). A further series of video frames is shown in figures 7 & 8. In figure 8 the solid lines approximately represent the edges of the vortices. Further to figure 6, in figure 8(c)-(e) the earlier leg intertwines with the leg of the later vortex. Later, the tornado vortex is formed attached to the flat plate adjacent to the cavity (figure 8(f)).

A vortex line representation is given in figure 12. Vortex lines approaching the cavity are initially parallel. The velocity within the cavity shear layer is higher than that within the boundary
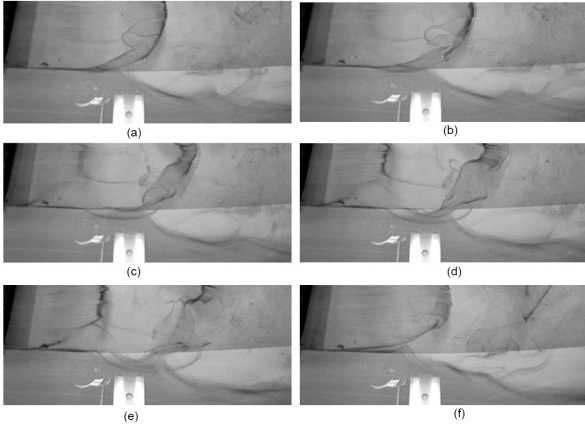
Figure 7: Series of video frames that show the interaction of the shear layer vortices. Similar (although expanded) field of view as 'Detail A' on figure 3. Parts (a) to (f) show increasing time. Flow is from left to right. There is a reflection from overhead lighting on the free surface of the water.

layer, causing the vorticity in the shear layer to travel faster relative to that in the neighbouring boundary layer. As the vortex lines bunch due to the shear layer instability, vortex loops form with streamwise-orientated legs. The initial deformation of the vortex lines causes each leg to then descend laterally down into the cavity due to the vortex induced velocity. These vortices are shown with their image pairs in figure 12(b). This behaviour is consistent with the identification of lateral in-flow in the upstream part of the cavity by Crook *et al.* [4].

Figure 12(b) shows how the spanwise roller curves and stretches, forming a half-ring which by self-induction will tend to convect higher, out of the cavity, as with the earlier vortex. Subsequently, the 'leg' of the earlier vortex interacts with the 'leg' of the later vortex as shown in figure 12(c). Shortly thereafter the vortices emerge over the sides of the cavity, with careful observation confirming that these features did indeed contain vorticity. (A possible explanation for the emergence is that the sharp corner of the vortex loop causes an increased rate of upward convection.) The side of the earlier vortex is then drawn into the later vortex (see figures 7 and 8), causing a region of velocity reversal on the floor, stretching and also uplift. This leads to the formation of a tornado vortex as in figure 12(d). The tornado vortex is in an unsteady sense anchored to the flat plate, as the anchor point continues to convect downstream with the flow. Note that, at a similar time to these events, the remainder of the shear layer vortex appears to become anchored to the inside side walls of the cavity.

Wind tunnel measurements

Velocity measurements were also taken in air using a single-wire hot wire probe, at a higher Reynolds number. Figure 9 shows a plan view of the velocity magnitude recorded near the flat plate surface and over the cavity, measured in a grid with streamwise spacing of 9mm and spanwise spacing of 3mm. The time-averaged flow properties appear to be reasonably symmetrical about the downstream portion of the cavity.

Figure 9 shows that regions of lower velocity magnitude and higher velocity fluctuation are found near each of the rear corners of the cavity. A cross-stream (lateral) view of this behaviour measured near the rear corner is shown in figure 10. Both profiles show that there is a region of low mean velocity and high velocity fluctuation immediately adjacent to the corner of the cavity. This behaviour may be related to low velocity fluid emerging laterally from the cavity, over the sides, forming a vortical feature. It is unclear whether these are related to the structures discussed earlier, being found further downstream due
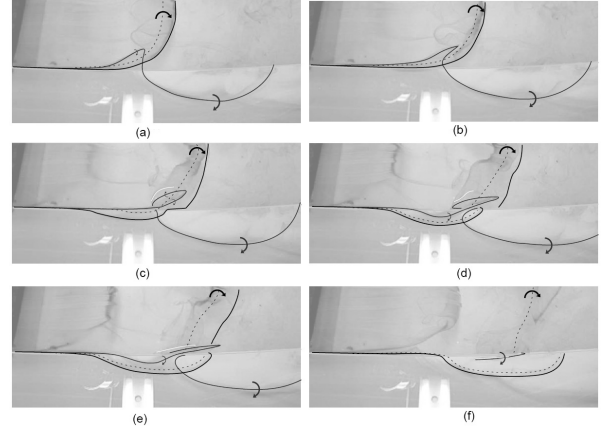

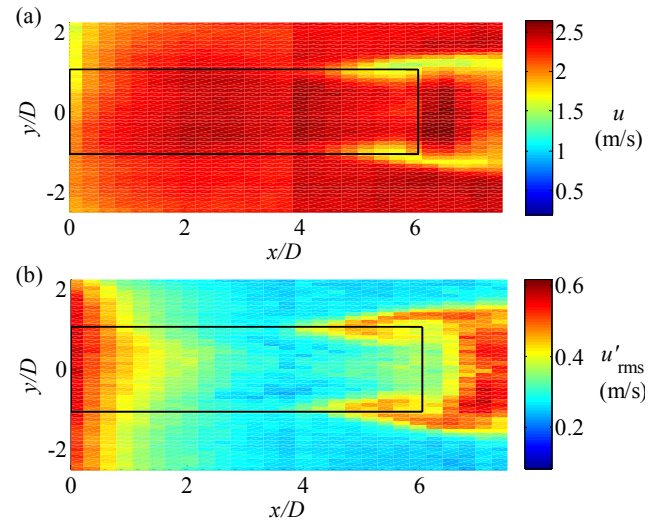Figure 8: Annotated version of figure 7.

Figure 9. Plan view of the cavity (indicated by black lines) with flow from left to right. (a) Local velocity magnitude. (b) Local root-mean-square fluctuation velocity. Measurement taken at height z/D=0.17.
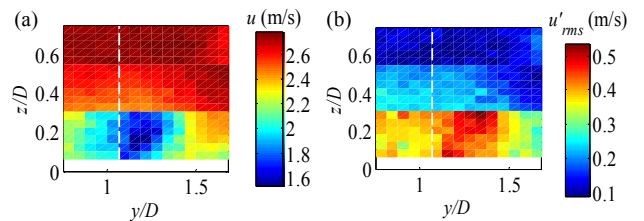

Figure 10. Cross stream view of velocity measurements near the rear corner of the cavity at x/D=6.07. The cavity is to the left of the dashed white line. (a) Mean velocity magnitude. (b) RMS fluctuation velocity.

to the higher Reynolds number in this case, or if they might be separate rear corner structures as suggested in figure 1 and also by Crook *et al.* [4].

Conclusions

Some original experimental observations on the flow structure at the sides of a three-dimensional cavity flow have been presented. A periodic structure forms which can be explained as an interaction of the stream-wise-orientated portions of successive shear layer vortices with the adjacent flat plate and the cavity side wall. In future work, it is hoped to study these structures and the overall cavity flow in more detail. Forcing will be applied to obtain a more regular flow structure and modified cavity geometries—a form of passive control—will be investigated.

References

[1] Ahuja, K K, and Mendoza, J, 1995, '*Effects of Cavity Dimensions, Boundary Layer and Temperature on Cavity Noise with Emphasis on Benchmark Data to Validate Computational Aeroacoustic Codes*', Tech. Report, NASA Contractor Report 4653.

[2] Atvars, K, Knowles, K, Ritchie, S A, and Lawson, S J, 2009, 'Experimental and computational investigation of an 'open' transonic cavity flow', *J. Aerospace Eng.*, vol. 223, pp. 357-368. doi:10.1243/09544100JAERO445

[3] Crook, S D, Hassan, E R, and Kelso, R M, 2008, 'Low Speed Cavity Flows: Principal Flow Features', In *Proceedings of the Fifth Australian Conference on Laser Diagnostics in Fluid Mechanics and Combustion*.

[4] Crook, S, Kelso, R, and Drobik, K, 2007, 'Aeroacoustics of Aircraft Cavities', In *Proceedings of the 16th Australasian Fluid Mechanics Conference*.

[5] Gursul, L, Lusseyran, D, and Rockwell, D, 1990, 'On interpretation of flow visualization of unsteady shear flows', *Exp. Fluids*, vol. 9 pp. 257-266.

[6] Knowles, K, Ritchie, S A, and Lawson, N J, 2007, 'An Experimental and Computational Investigation of a 3D, l/h=5 Transonic Cavity Flow', In *Proceedings of 3rd International Symposium on Integrating CFD and Experiments in Aerodynamics*.

[7] Lasheras, J C, and Choi, H, 1988, 'Three-dimensional instability of a plane free shear layer: an experimental study of the formation and evolution of streamwise vortices', *J. Fluid Mech.*, vol. 189, pp. 53-86.

[8] Rockwell, D, and Knisely, C, 1983, 'Observations of three-dimensional nature of unstable flow past a cavity', *Phys. Fluids*, vol. 23, no. 3, pp. 425-431.

[9] Zhang, K, and Naguib, A M, 2011, 'Effect of finite cavity width on flow oscillation in a low Mach-number cavity flow', *Exp. Fluids*, vol. 51 pp. 1209-1229.
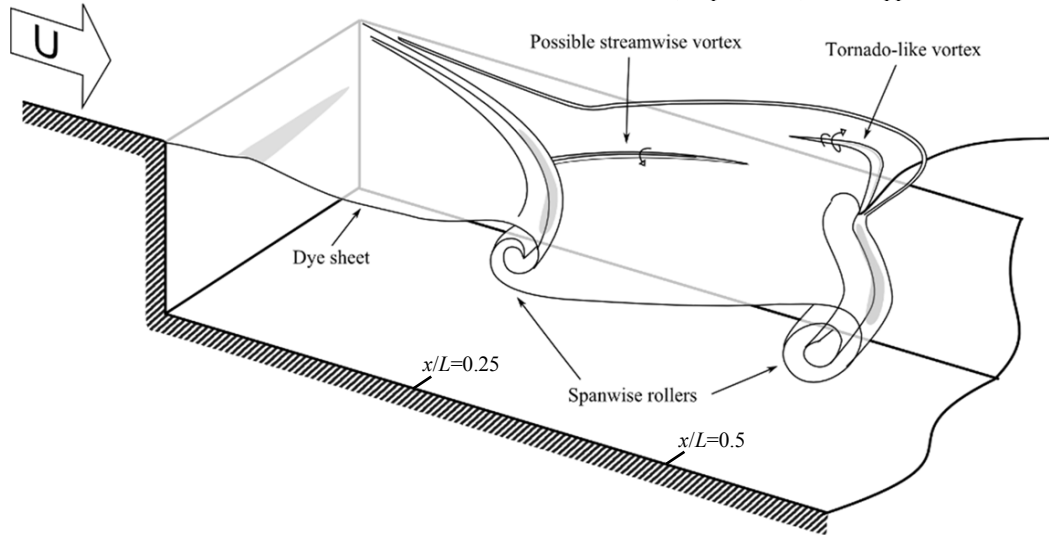
Figure 11: Cut-away sketch of instantaneous dye visualization pattern when dye was released from a slot in the plate upstream of the cavity at Re_D = 2700. The sketch is cut at half the width of the cavity. The observed pattern was symmetrical about this plane.
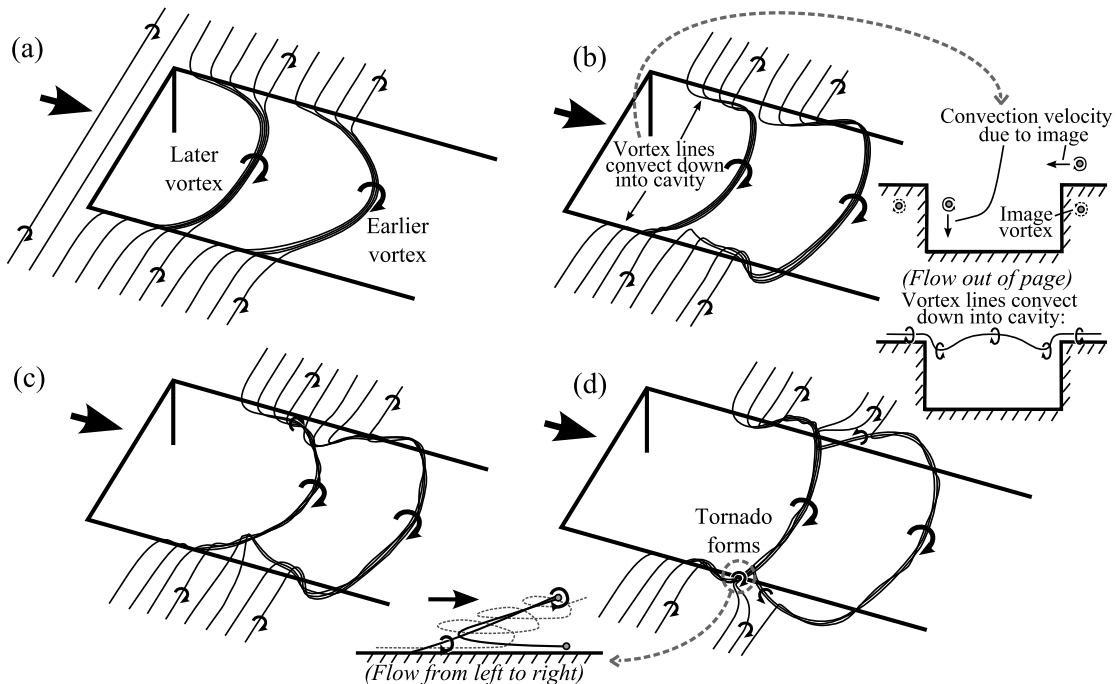

Figure 12: Vortex line representation.